

Improved representation of convective moistening in JMA's next-generation coupled seasonal prediction system

KOMORI Takuya*, HIRAHARA Shoji and SEKIGUCHI Ryohei
Climate Prediction Division, Japan Meteorological Agency, Tokyo, Japan
Email: komori@met.kishou.go.jp

1. Introduction

The Japan Meteorological Agency (JMA) is developing the next-generation Coupled Seasonal Ensemble Prediction System version 3 (JMA/MRI-CPS3; CPS3), which consists of 60km atmospheric components and an eddy-permitting (0.25 deg.) ocean component. In addition to supporting three-month, warm-/cold-season and El Niño forecasts, CPS3 will provide sea surface temperature (SST) data as a lower boundary condition in JMA's Global Ensemble Prediction System (GEPS) for a two-tiered SST approach (Takakura and Komori, 2020). Since GEPS supports the issuance of operational typhoon information as well as one-week, two-week and one-month forecasts, CPS3 prediction skill in light of the link between operational weather and climate predictions is crucial. This report details results from verification of convective moistening in CPS3.

2. Revised convection scheme in CPS3

CPS3 involves the use of the prognostic Arakawa-Schubert convection scheme with a spectral cloud ensemble and prognostic closure with certain modifications (JMA 2019). The scheme is revised after Komori and Shimpo (2016) with modifications focusing on moistening processes in the tropics:

- a) Introduction of relative humidity (RH)-dependent formulation inspired by Bechtold et al. (2008) for entrainment $\varepsilon(z, t, i)$ in updraft mass flux:

$$\begin{aligned}\varepsilon(z, t, i) &= \varepsilon'(t, i) f(\overline{RH}(z)) \\ f(\overline{RH}(z)) &= \left((RH_c - 1) \frac{\bar{q}_s(z)}{\bar{q}(z)} + \frac{\bar{q}_s(z) - \bar{q}(z)}{\bar{q}(z)} \right) \times \left(\frac{\bar{q}_s(z)}{\bar{q}_s(z_B)} \right)^\alpha \\ &= \left(\frac{RH_c - \overline{RH}(z)}{\overline{RH}(z)} \right) \times \left(\frac{\bar{q}_s(z)}{\bar{q}_s(z_B)} \right)^\alpha\end{aligned}$$

Here, the constant parameter $RH_c = 1.1$, and $\varepsilon'(t, i)$ is diagnosed for each convective plume i at every time step t depending on the environmental profile of moist static energy. \bar{q} and \bar{q}_s are specific humidity and saturation specific humidity in the environment, respectively. z_B is the convective cloud bottom height, and α is a constant.

- b) Loosening of the upper limit of the entrainment rate for shallow convection with cloud top lower than 700 hPa.

3. Experimental configuration and results

The current configuration of CPS3 (TEST) was compared to the configuration without the revision of the convection scheme (CNTL) in three experiments with different forecast ranges and model resolutions. Verification of 72-hour forecasting against the RH of ERA5 reanalysis (Hersbach et al., 2020) and GPCP precipitation (using the atmospheric component of CPS3 with 120-km resolution) in July and August 2009 showed that the convection scheme revision significantly improved vertical RH profiles depending on precipitation over the Indian Ocean (Figure 1). As expected, the normalized number of precipitation occurrences was also improved as a result of better convective moistening due to the effect of RH-dependent entrainment.

In relation to medium-range forecasting, error growth for the specific humidity profile in the tropics was also verified against radiosonde observation during the 11-day forecast in an experiment on analysis (data assimilation) and forecast cycles in August 2018 using the atmospheric component of CPS3 with 20km resolution. The results demonstrated that TEST outperformed CNTL with less bias and smaller error growth (Figure 2).

As a verification of convectively coupled equatorial waves in long-range forecasts, wavenumber-frequency spectra with an equatorially symmetric component of the OLR (simulated over the period from 2001 to 2007 using the atmosphere-ocean coupled model with the same resolution as CPS3) showed TEST improved the too small amplitude and too high frequency of Kelvin wave in CNTL, as compared to NOAA AVHRR satellite observation (Figure 3). Overall, the revision of the convection scheme showed encouraging results with significant improvement of prediction for many aspects of moistening processes in tropics.

REFERENCE

- Bechtold P., M. Kohler, T. Jung, F. Doblas-Reyes, M. Leutbecher, M. Rodwell, F. Vitart and G. Balsamo, 2008: Advances in simulating atmospheric variability with the ECMWF model: From synoptic to decadal timescales. *Q. J. R. Meteorol. Soc.*, **134**, 1337–1351.
- Hersbach, H., B. Bell, P. Berrisford, S. Hirahara, András Horányi, J. Muñoz-Sabater, J. Nicolas, C. Peubey, R. Radu, D. Schepers, A. Simmons, C. Soci, S. Abdalla, X. Abellan, G. Balsamo, P. Bechtold, G. Biavati, J. Bidlot, M. Bonavita, G. De Chiara, P. Dahlgren, D. Dee, M.

Diamantakis, R. Dragani, J. Flemming, R. Forbes, M. Fuentes, A. Geer, L. Haimberger, S. Healy, R.J. Hogan1, E. Hólm, M. Janisková, S. Keeley, P. Laloyaux, P. Lopez, G. Radnoti, P. de Rosnay, I. Rozum, F. Vamborg, S. Villaume and J.-N. Thépaut, 2020: The ERA5 Global Reanalysis. *Q. J. R. Meteorol. Soc.*, accepted.

Komori, T. and A. Shimpo, 2016: Improvement of MJO prediction and moistening processes for the DYNAMO period. *CAS/JSC WGNE Research Activities in Atmospheric and Oceanic Modeling*, 4.05-4.06.

Takakura, T and T. Komori, 2020: Two-tiered sea surface temperature approach implemented to JMA's Global Ensemble Prediction System. *CAS/JSC WGNE Research Activities in Atmospheric and Oceanic Modeling*, submitted.

JMA, 2019: Outline of the operational numerical weather prediction at the Japan Meteorological Agency. Appendix to WMO technical progress report on the global data-processing and forecasting system and numerical weather prediction research. 188pp. Available online: <http://www.jma.go.jp/jma/jma-eng/jma-center/nwp/outline2019-nwp/index.htm>

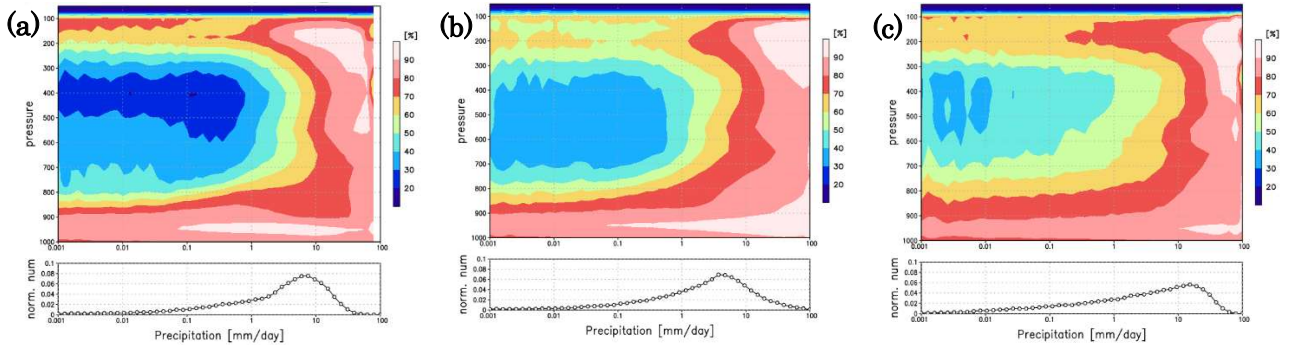


Figure 1. Vertical RH profiles [%] (shading) depending on precipitation [mm/day] averaged over 72-hour forecasts using the atmospheric component of CPS3 in July and August 2009 over the Indian Ocean for (a) CNTL and (b) TEST with reference to (c) ERA5 and GPCC. The normalized number of precipitation occurrences is shown in the bottom figure.

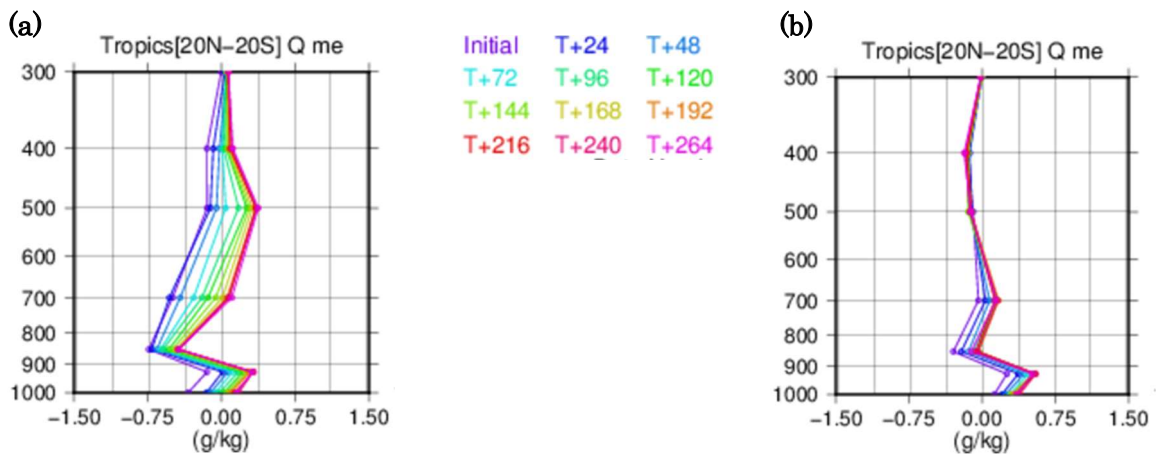


Figure 2. Forecast error growth for specific humidity [g/kg] averaged over the tropics (20°S – 20°N) in an analysis-and-forecast cycle experiment using the atmospheric component of CPS3 with 20km resolution: (a) CNTL and (b) TEST. Colored profiles show forecast errors against radiosonde observations at each forecast time averaged over August 2018.

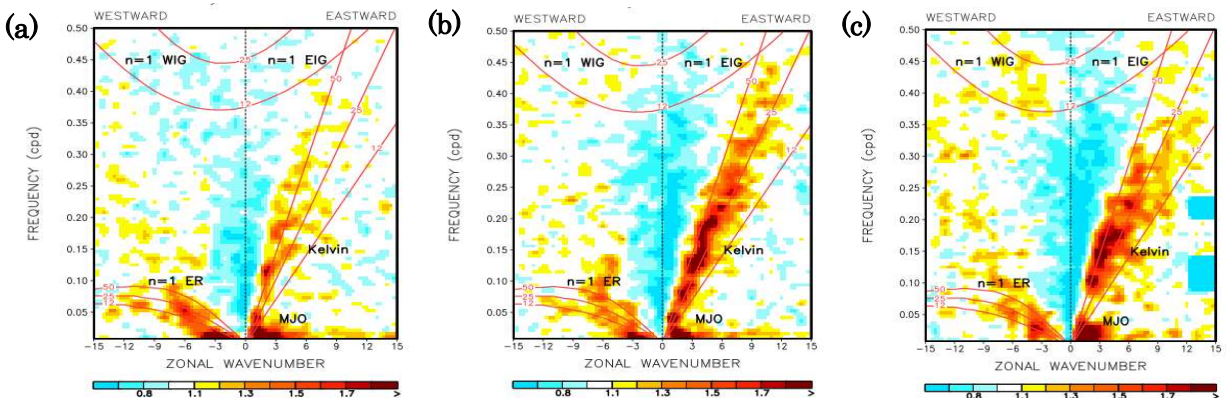


Figure 3. Wavenumber-frequency power spectra with an equatorially symmetric component of the OLR (15°N – 15°S) in experiments using the atmosphere-ocean coupled model with the same resolution as CPS3: (a) CNTL, (b) TEST and (c) NOAA AVHRR satellite observation from 2001 to 2007.